Electrical Engineering (2023) 105:3191–3208
https://doi.org/10.1007/s00202-023-01843-1

ORIGINAL PAPER


# A non-PMU-based WAN protection scheme for swing detection and stability enhancement in power systems

**Ehab A. El-Metwally[1] · Mahmoud A. Attia[1] · Mohamed El-Shimy[1]**

Received: 25 October 2022 / Accepted: 19 April 2023 / Published online: 4 June 2023


**Abstract**
This paper presents a scheme for power swing detection and stability assessment for multi-machine power systems in addition to a brief survey on that topic. The scheme adopts smart grid perception. It is an asynchronous scheme that uses the rate of change of the angle of the generator bus voltage instead of synchronously estimating the absolute rotor angle value for stability assessment. Therefore, it does not require phasor measurement units (PMUs). Instead, it uses commercially available intelligent electronic devices (IEDs). It introduces a new application of the multicast Generic Object Oriented Substation Event (GOOSE) protocol or its routable version (R-GOOSE) to reflect the disturbance in the power grid on the transmission pattern of data packets over the grid data network. In this scheme, the angle change information is transmitted in the form of GOOSE packets simultaneously from the IEDs that readily measure the angles of the affected generators. On the other hand, the detecting device identifies the stability status of each affected generator. The proposed scheme is validated by simulating disturbances on the IEEE 39-bus system. The results show that the scheme can discriminate between stable and unstable swings. In addition, the loss of synchronism of the unstable generator is predicted ahead of its occurrence by enough time to take an appropriate action.

**Keywords** Power swing · Rotor angle stability · Protection relays · IEC 61850 · GOOSE · R-GOOSE · Smart grid

## Abbreviations

| | |
|---|---|
| AI | Artificial intelligence |
| ANN | Artificial neural network |
| AR | Auto-regression |
| DFT | Discrete Fourier transform |
| EAC | Equal area criteria |
| GMDH | Group method of data handling |
| GOOSE | Generic Object Oriented Substation Event |
| IED | Intelligent electronic device |
| LAN | Local area network |
| MLE | Maximal Lyapunov exponent |
| MAC | Medium access control |
| MDGP | Most disturbed generator pair |
| PC | Personal computer |
| PMU | Phasor measurement unit |
| R-GOOSE | Routable GOOSE |
| RIAC | Rate of impedance angle change |
| SCL | Substation configuration language |
| SCV | Swing center voltage |
| SDGP | Severely disturbed generator pair |
| UDP/IP | User datagram protocol/Internet protocol |
| UTC | Universal coordinated time |
| WAMPAC | Wide area monitoring, protection and control |
| WAMS | Wide area measurement system |
| WAN | Wide area network |

✉ Ehab A. El-Metwally
ehab.state@yahoo.com

Mahmoud A. Attia
mahmoud.abdullah@eng.asu.edu.eg

Mohamed El-Shimy
mohamed_bekhet@eng.asu.edu.eg

[1] Faculty of Engineering, Ain Shams University, 1 Elsarayat St., Abbaseya, Cairo 11517, Egypt

## 1 Introduction

Under steady-state conditions, the electrical grid operates very close to its nominal frequency (± 0.5%) and normally keeps absolute voltage differences between buses around 5%. This steady state is due to the balance between generated

and consumed active and reactive powers. Faults as well as some operative or protective actions such as line switching, sudden load changes, outage of generators and other actions which are common and inevitable in power systems may result in sudden disturbances in power flow. Depending on how severe they are, these disturbances produce transients in the power systems and may affect system stability. Furthermore, a minor disruption may be enough to trigger a blackout or brownout due to the fact that modern power systems operate closer to their stability limitations for economic reasons [1]. The stability in this situation depends on whether the resulting transient oscillations damp with time or not. If the transient oscillations damp with time, then the major portion of the power grid will transfer to a new steady-state operating condition. On the other hand, if the oscillations persist with time, then the system might become unstable or out of step.

Different methods for power swing detection and stability assessment are presented in the following section.

### 1.1 Overview of existing power swing detection techniques

The legacy-applied techniques of power swing detection and out-of-step protection rely on measurements of electrical parameters. The most widely used parameter is the impedance, where its rate of change is directly proportional to the swing frequency according to [2]. The out-of-step and stable power swing conditions are discriminated further based on the monotonicity of the impedance change. Figure 1 shows the rate of change of impedance method.

In [3, 4], the blinder technique is introduced. The measured impedance in this technique is the load impedance under typical system operating conditions, and its locus is normally away from the distance relay protection characteristics. When a fault occurs, the measured impedance moves almost instantaneously from the load impedance point to the point that corresponds to the fault in the impedance plane. Under swing condition, the measured impedance on the impedance plane moves in a slow pace on the impedance plane. Figure 2 shows the blinder scheme.

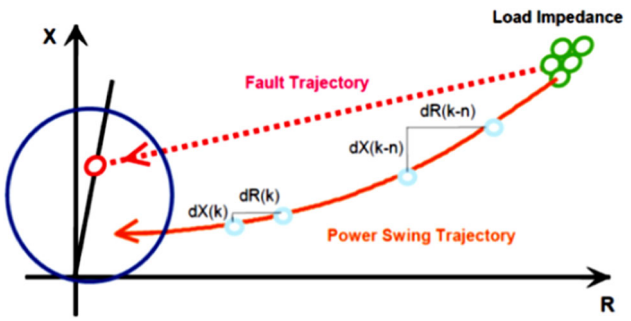


**Fig. 1** Swing detection based on rate of change of impedance

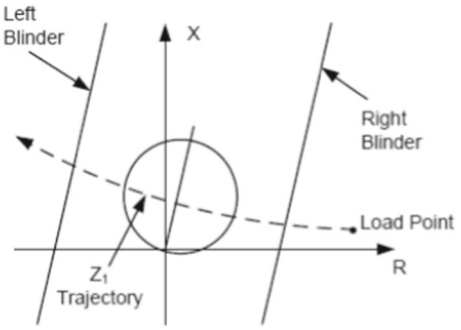


**Fig. 2** Single blinder scheme characteristics

The main drawback of the blinder technique is the fact that extensive offline stability simulations for various swing scenarios are necessary for setting the impedance blinders; in addition, it is not suitable to detect swings of increasing frequency slips. Moreover, it is a local swing detection, confined to the protection connection point, and this scheme is mainly used to discriminate the power swing from fault condition in distance relays. As a modification to the rate of change of impedance method, *the rate of change of apparent resistance* is introduced in [5]. For the purpose of out-of-step detection, the study domain and the electrical parameters used are changed. Nonetheless, this method offers no advantages over rate-of-change impedance-based approaches.

Another conventional out-of-step detection method is *the swing center voltage (SCV)* technique [6], and it computes voltage at a virtual center in the power system. When the angles between the two sources of a two-source equivalent system are 180 degrees apart, there is a location in the network with zero voltage. The voltage at this location at different angle values is defined as the SCV. The SCV method utilizes the voltage change rate at the swing center to decide whether out-of-step condition is valid or not [2–7]. The main drawback of the SCV method is that it is applicable only on the two-machine system; therefore, their implementation in actual multi-machine power systems requires extensive network reduction. Moreover, the estimation of voltage at the virtual center is accurate only when the line impedance angle is 90 °.

The authors of [8] proposed a *coordination transformation* scheme for swing detection using a two-machine equivalent system; however, several empirical thresholds are used for multi-machine power systems, which requires offline studies. The authors of [9] proposed the study of the trajectory on state plane to determine the critical clearing time and angle based on estimation of total energy. However, reducing the entire network to the equivalent two-area system is necessary for this method.

A non-conventional swing detection scheme called *continuous impedance calculation* is introduced in [10]. It entails tracking the trajectory of three modified loop impedances in

the complex plane. The criteria of power swing are met when the change in all three-loop impedances fulfills continuity, monotony and smoothness. A major advantage of the continuous impedance calculation is the fact that no settings are required and therefore it does not require any stability studies involving complex simulations, while the limitation is the fact that it is a local swing detection, confined to the protection connection point. Besides, the scheme is not applied by all relay manufacturers.

In [11], an algorithm for power swing detection based on the rate of change of impedance angle is proposed. The algorithm defines an index for measuring the impedance angle and another index for the rate of impedance angle change (RIAC). The RIAC index is used to discriminate fault from power swing, while the impedance angle index is used to identify the out-of-step condition during the power swing. The algorithm is fast and can be implemented in industrial relays; however, it is still local detection like the above-mentioned schemes.

The authors of [12] proposed a scheme for power swing detection and distance relay blocking using the *variance calculation of the current sampled data*. In a way to reduce computations, burden in a digital relay is to perform them directly on the sampled data. The proposed algorithm calculated the variance of discrete data of the three phase currents by averaging the square of the predicted or observed distance from the expected value. Since the variance is a measure of how a series of data are spread around their mean value, it can be used as a distinguishing parameter of the disturbance whether it is a fault or a swing. The changes in the variance value during power swings are small, but during a fault, these changes are extensively large. Accordingly, a threshold is calculated to distinguish the power swing from the fault case. The main drawback of this method is that the threshold value required by the scheme must be obtained using variety of power swing types and variety of fault types. Also, it is a local swing detection, confined to the protection connection point; therefore, it is mainly used to discriminate the power swing from fault condition in distance relays. Moreover, the scheme needs to be proven by industrial relay manufacturers.

Intelligence-based methods for protection against out-of-step were also proposed [13–20]. A scheme based on *fuzzy logic* was introduced in [13] for out-of-step detection. The inputs used in the fuzzy inference blocks comprise measurements such as pre-fault and post-fault currents, voltages and the generators angular speeds. However, the out-of-step detection effectiveness is only demonstrated for a two-machine power system.

The authors of [17] used fuzzy logic to identify out-of-step conditions by utilizing phasor measurements. However, when used on big multi-machine power systems, the main challenges are identifying adequate input variables, membership functions and creating appropriate "if–then" decision rules.

*Artificial neural network (ANN)*-based approach was introduced by the authors of [14, 15] for out-of-step protection. Nevertheless, this approach was verified for systems comprising up to three machines only. In [20], a new ANN approach using the *group method of data handling (GMDH)* was introduced. The GMDH approach is better performing and requires less training time compared with other conventional neural networks. The response time of this approach is good, yet it requires the distance protection function to operate during detection. Besides, in principle, substantial offline simulations are necessary for ANN based approaches to train and test the algorithm. In [21], *equal area criteria (EAC)* in$P$–$\delta$ curve is applied to detect out-of-step condition. According to the EAC-based method, the initial power angle and the critical clearing angle ($\delta_{cr}$) are calculated and the accelerating area under the $P$–$\delta$ curve following a fault is compared with the decelerating area following the fault clearance to determine whether an out-of-step condition occurs. The EAC method's primary flaw is that multi-machine power systems cannot be directly applied to it. The EAC approach is applied right away to a multi-machine power system in [22–25] without network reduction and is adjusted to work in the time domain. However, [22–25] use numerical simulation of only few chosen case studies to illustrate the suggested algorithm in multi-machine systems. The authors of [26] introduce an extended EAC (EEAC) that can be used for out-of-step detection in multi-machine systems. However, it reduces the multi-machine system to an equivalent two-area system. So, in the EEAC method, network reduction is still crucial, leading to system-specific settings for out-of-step detection.

With the advent of phasor measurement units (PMUs), the protection system of power grid was able to utilize the information contained in wide area measurement system (WAMS) and hence novel out-of-step protection algorithms could be invented.

*Lyapunov's method* has been successfully used for stability investigations in power systems [27, 28]. PMU-based out-of-step detection that uses dynamic state estimation and Lyapunov functions was developed by the authors of [29]; however, the technique is only realized for the two-area equivalent system. In an attempt to achieve a stability region that is similar to Lyapunov's direct technique, Zubov developed a modified method using approximations. Studies of power systems stability have employed *Zubov's method*; however, protection applications have not. In [30], Zubov's approximate stability boundaries were used for out-of-step detection application. The detection method used a group of those Zubov's stability boundaries in power angle–frequency ($\Delta$–$\omega$) plane. The proposed algorithm is based on real-time

PMU measurements and can be readily implemented for multi-machine power systems without requiring extensive offline simulation studies/network reduction for out-of-step settings. Zubov's boundaries are computed given the information of $\delta_0$ and $\omega_0$ information, which can be obtained from measurement units placed on the power grids. Continuous PMU data streaming is received during the disturbance and utilized to plot trajectories on $\delta$–$\omega$ plane. For out-of-step detection, the $\delta$–$\omega$ trajectory must pass through the outermost boundary [30].

Case studies are carried out with this scheme in SMIB and New England 10-machine 39-bus power systems and showed good results. The main drawback of this method is that the boundaries are predefined based on initial operating condition and are not updated in real time according to load changes.

Another wide area PMU-based scheme in wide area network power swing detection was introduced in [31]. A *maximal Lyapunov exponent (MLE)-based model-free* rotor angle stability assessment approach is proposed. In order to measure the stability of dynamic systems, Lyapunov exponents (LEs), which describe the separation rate of infinitesimally close trajectories, are considered strong indicators. The system is unstable if its maximal Lyapunov exponent (MLE) is positive, and vice versa. Model-free LE-based stability assessment techniques were adopted as they can reduce calculation complexity and avoid model errors; however, a time window must be identified for MLE monitoring purpose. For fast and accurate evaluation of stability, the window size is essential. The scheme relies on determining the severely disturbed generator pairs (SDGPs) as they are the main factor controlling system dynamics following significant disturbances. The SDGP's relative rotor speed and the separation between the rotor angle trajectories are closely related. MLE is estimated for SDGP rotor angle trajectory. Real-time measurements of the rotor speed and relative rotor angle are collected by PMUs.

When the MLE curve of an SDGP is estimated, the assessment of rotor angle stability depends on the pattern of that curve, either increasing or decreasing with time. The system is considered stable if all SDGPs are stable; otherwise, the system is unstable. The main drawback in this method is the fact that the scheme needs relatively long time for the MLE estimation process to be completed, which is not adequate for detection of fast swings.

The authors of [32] proposed a method for assessing rotor angle stability using WAMS data. The method identifies the generator pair that is most adversely impacted by a disturbance by evaluating rotor angle deviations. According to [33], a system of a group of generators becomes angle unstable when a pair of generators have an angle difference of 180° or more between them. In [32], relative rotor angle between each generator pair is defined as the angle between each pair of machines at any time instant after disturbance. Relative angle between the same pair of machines just before disturbance is also defined. The generator angles are estimated with respect to the slack bus generator. PMUs measurements and streaming are used for the estimation of the generators' rotor angles. Most disturbed generator pair (MDGP) is identified from the two defined relative angles for each generator pair. Stability assessment is then applied on the identified most disturbed generator (MDG) using a predictive auto-regression (AR) approach to identify unstable fast swing if the predicted value crosses a threshold. For slow swing, the damping coefficient of the most dominant frequency obtained from Prony analysis is used in conjunction with the instantaneous rotor angle values to obtain a stability index. The results show improved performance compared to the MLE approach in [31] in detecting fast swings.

A more recent technique is to apply machine learning and big data obtained from PMU-based WAMS system in stability assessment. In [34], a scheme based on big data and core vector machine was introduced to realize real-time calculations on overwhelming datasets. However, multi-stage offline training procedure is essentially required which increases complexity and time consumption and renders the accuracy of such schemes subject to the availability of very large amount of data. In addition, the adversarial examples are serious challenge to the machine learning approach in general which requires to be mitigated. Adversarial examples are inputs to a neural network that result in an incorrect output from the network. In [35], a mitigation model was proposed for the vulnerability of machine learning-based power system stability assessment under adversarial examples. However, the machine learning approach still needs more advancements to match power systems requirements.

In summary, it could be said that all the existing methods used in power swing detection and stability assessment are either local methods built in an individual device or require long offline stability simulations like in conventional impedance-based methods or consume long time for data gathering and training like in AI-based and machine learning-based methods. Furthermore, for the existing WAMS-based stability assessment methods, the absolute value of the rotor angle of some selected generators on the grid is estimated using synchrophasors calculated by PMUs. Thus, an additional device other than the normally existing devices in the power plant has to be placed at each selected generator node on the grid. Also, these schemes require continuous transmission of the estimated rotor angle whether there is a swing or not, and this may increase statistically the vulnerability to noise and errors. In addition, the PMUs have to synchronize their measurements using a time reference like a GPS clock, which adds to the restrictions of the existing WAMS-based schemes. It is also worth to mention that the available WAMS-based mathematical algorithms to evaluate

stability are not standardized, as there are diverse mathematical approaches adopted by researchers and hence are not applied—so far—in the industrial level.

### 1.2 Objectives of the proposed scheme

In this paper, a new scheme for power swing detection in multi-machine power systems that uses packet switched network industrial protocols is proposed. It adopts the smart grid concept which calls for expanded use of digital information and controls technology to enhance the electric power grid's reliability, security and efficiency. The scheme aims to overcome the above-mentioned restrictions in the current techniques, especially the WAMS-based ones. This is accomplished by introducing the concept of asynchronous estimation of the change in rotor angle instead of the synchronous estimation of absolute rotor angle using PMUs. This is certainly achievable in the scheme since it relies on estimating the change of each generator rotor angle with respect to its own initial value, not on the angle absolute value.

By asynchronous estimation, we mean that the voltage angle at any bus on the grid is measured by an intelligent electronic device (IED) independently and not synchronized to the measurements at other buses. The IED can be the existing protective relay that normally measures the bus voltage and hence can compute the phase angle and reflect its change on the pattern of data it transmits on the network. This approach will replace estimating the absolute value of each generator angle via a PMU synchronously with other PMUs connected to the selected grid buses and sending the estimated data continuously whether there is a change in the angle or not, as in the WAMS technique.

Thus, the data transmission in the proposed scheme will be restricted to the power swing period and hence will reduce the traffic on the communication network and consequently vulnerability to errors. Last, the proposed scheme presents an approach to standardize the process of grid stability assessment by applying international industrial communication standards instead of applying diverse schemes involving various mathematical methods.

The rest of this paper is divided into three sections. Section 2 introduces the proposed scheme. Section 2.1 presents the basic operation principle. Section 2.2 introduces the concept of estimating the change in rotor angle in terms of change in the generator bus angle. Section 2.3 demonstrates the process of phase angle estimation as implemented in numerical relays. Section 2.4 illustrates the concept of transmission of phase angle change information in a coded form on the network when the angle exceeds predefined limits. Section 2.5 illustrates the concept of measuring a perturbation in a system using the GOOSE protocol. Section 4 shows the simulation results for fast unstable and stable swing cases, which proves the fast detection capability of the proposed scheme. Finally, the conclusion is presented in Sect. 4.

## 2 The proposed scheme

In this section, the proposed scheme is introduced. The principle of operation of the scheme and the important contributions are presented in Sect. 2.1. In Sect. 2.2, it will be proven that the rate of change of rotor angle of the generator is the same rate of change in generator bus voltage angle and consequently the latter will be used in this work for stability assessment. In Sect. 2.3, the method of computing the change in generator bus voltage angle during power swing condition will be shown using the discrete Fourier transform (DFT) adopted in numerical IEDs. In Sect. 2.4, the concept of mapping the change in bus voltage angle (obtained in Sect. 2.3) to Boolean variables will be is presented. In addition, the transmission principle of Boolean variables via multicast network protocol is demonstrated. In Sect. 2.5, it will be proven that the multicast GOOSE or R-GOOSE protocols are the appropriate protocols to transmit the mapped Boolean variables and that their operation mechanism can be used to detect the perturbation in the generator bus voltage angle and hence the perturbation in generator rotor angle.

### 2.1 Basic operation principle

Following the major smart grid concept of increased employment of digital information and controls technology to improve the power grid reliability, the proposed scheme is developed.

For a cluster of interconnected generators in the grid as shown in Fig. 3, it is essential that each generator bus is connected to an IED that computes the bus voltage magnitude and angle. This normally existing IED will be used in the case of power swing to compute the angle change of the generator node suffering swing and transmit it in a coded or keyed form on a wide area network to one central detecting device (or more if needed). Since all modern IEDs can communicate using IEC 61850 standard and almost all power grids possess fiber optic cables that enable very high-speed data communications, the power grid data network can be used to transmit specific protocol data packets, indicating the swing rate in direct proportionality to the rate of change of the measured bus voltage angle.

The central detection node of that cluster (with IED 1 in Fig. 3) will receive the multicast protocol messages and detect the swing severity at the sending generator node based on a certain algorithm. It can react accordingly to each point suffering swing with the appropriate action through the same protocol. Thanks to the very high speed of the data network multicast protocol, the central detection IED can receive the

messages from all nodes simultaneously without the need of synchronizing the measurements at all nodes like the PMU synchrophasor technique.

The most important contributions of the proposed scheme are:

- In comparison with traditional or legacy methods:
- It is a wide area scheme that has a central device for stability assessment and hence avoids the drawbacks of local single node decisions that may entail adverse impact on the grid as the response might differ from one device manufacturer to another
- It relies on evaluating the rate of change of rotor angle which is the main parameter in the swing phenomenon, but it does not measure a dependent electrical parameter (like the impedance)
- It does not need network reduction methods to evaluate stability since the actual rotor angle rate of change is readily available simultaneously for all network nodes
- In comparison with the existing WAMS-based methods:
- The rotor angle change is estimated asynchronously in the generator bus IED; thus, it does not require synchronized sampling at all nodes
- It does not need additional measuring devices like PMUs to be connected to the grid nodes as it utilizes the already existing IEDs in the power plant to compute the phasor angle of the generator bus voltage in the same way the PMU does, but without synchronization
- It uses industrial proven communication protocols applicable to today's protection devices
- It does not require continuous transmission of absolute values of angular frequency ($\omega$) and/or phase angle ($\delta$), which minimizes traffic burden on the network and statistically reduces the vulnerability to noise and errors

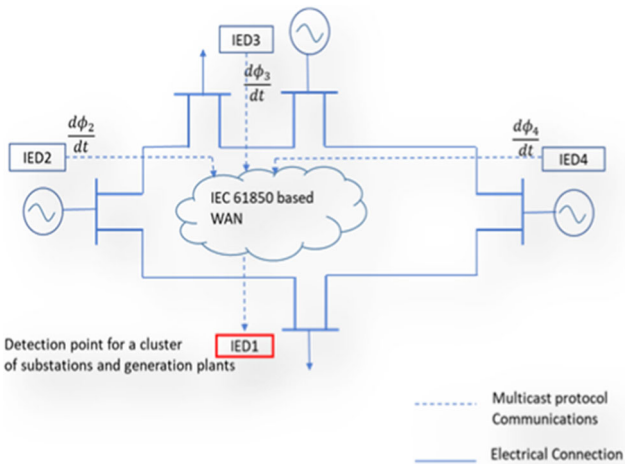


**Fig. 3** The proposed wide area network scheme architecture

It is an approach to standardize the process of grid stability assessment by using standard industrial network protocols instead of using diverse mathematical algorithms.

## 2.2 Estimation of rotor angle change in terms of generator bus voltage angle change

The traditional approach in evaluating rotor angle stability in most of wide area detection schemes was to estimate the absolute value of the rotor angle of some selected generators on the grid using synchrophasors calculated by PMUs. The computed phase of the synchrophasor of each selected generator is then transmitted continuously to a central processing device to be compared synchronously to the corresponding phase of other generators on the grid, and hence the grid stability is evaluated. In this section, it will be proven that the rate of change of the rotor angle of each selected individual generator could be used to evaluate stability when computed simultaneously with that of other generators. The simultaneous computation does not require synchronized measurements, it will be rather done via real-time high-speed network communications.

In this section, we will show mathematically that the rate of change of the rotor angle can be determined in terms of the rate of change of the generator bus voltage angle.

Assuming a varying frequency with time such as in the case of accelerating machine rotor, the instantaneous phase difference between the varying frequency voltage signal and the constant frequency voltage signal is:

$$\Delta\emptyset_i = \int_0^t \Delta\omega(t)\mathrm{d}t \tag{1}$$

where $\Delta\Phi_i$ is the instantaneous phase shift from the constant frequency signal and $\Delta\omega$ is the angular frequency change in rad/s.

Differentiating both sides of (1) yields:

$$\frac{d\Delta\emptyset i(t)}{dt} = \Delta\omega(t) \tag{2}$$

Equation (2) reveals that the rate of change of the phase shift equals the instantaneous frequency deviation. It can then be concluded that when the angular frequency deviation becomes zero, the equation becomes:

$$\frac{d\Delta\emptyset i(t)}{dt} = 0 \tag{3}$$

Equation (3) implies that the phase shift becomes a constant value with time when the voltage signal frequency reverts to its nominal value. This condition holds when the

generator rotor reverts to its nominal speed and hence indicates the onset of oscillations.

At steady state, the generator's rotor is rotating with the nominal synchronous speed $\omega_0$ and the rotor angle $\delta$ is constant. However, when a disturbance occurs to the system like a fault or a sudden load rejection, the rotor accelerates and $\delta$ increases with time. As a result of this acceleration, the instantaneous phase angle of the generator bus voltage increases also with time. In a similar argument, after the fault clearance or load restoration, the rotor decelerates (while $\delta$ is still increasing) till the rotor speed reaches $\omega_0$ and then $\delta$ starts to decrease. In the latter case, the instantaneous phase angle of the generator bus voltage also follows $\delta$ in its behavior.

It can be shown that the instantaneous change in rotor angle from the nominal angle $\delta_0$ is given by [28]:

$$\frac{d\Delta\delta}{dt} = \Delta\omega(t) \tag{4}$$

From Eqs. (2) and (4), it can be seen that the rate of change in the instantaneous phase of the generator bus voltage is the same rate of change in the rotor angle:

$$\frac{d\Delta\emptyset i}{dt} = \frac{d\Delta\delta}{dt} \tag{5}$$

Therefore, the estimated change in the phase angle of the generator bus voltage can be used to indicate the change in the rotor angle and hence the status of the generator from rotor angle stability perspective.

### 2.3 Numerical phase angle estimation

Instead of using PMUs in the electrical grids to compute the voltage phase angle, in the proposed approach, the inherent function of the phase angle estimation of phasors in any numerical IED will be exploited. The sampling process to extract the phasors is typical in both PMUs and other IEDs like numerical relays; however, the sampling in numerical relays is not synchronized to a time reference as it is the case in the PMUs.

In this section, we will start with the concept of numerical extraction of the phase angle of voltage phasors to reach a mathematical expression for the change in voltage angle as frequency deviates from its nominal value during power swing.

Mostly, all numerical relays as well as PMUs adopt the discrete Fourier transform to extract the phasor of the measured voltage signal.

In the modern numerical protection relays involving digital signal processing, the computations are performed in the discrete-time domain.

Discrete signal is created by taking samples of a given continuous signal at specific instants of time.

The finite length sequence $x[n]$ now exists for a total number of samples $N$. The truncation of the signal into a limited number of samples $x[n]$ yields the DFT whose general formulation is given by:

$$X(k) = \sum_{n=0}^{N-1} x[n] e^{\frac{-j2\pi}{N}nk}, \quad n \le k \le N-1 \tag{6}$$

where $n$ is the sample number and $k$ is the harmonic frequency order.

Evaluating $X(k)$ at the fundamental frequency $f_0$ (corresponding to $k = 1$ in Eq. (14)) gives $X(1)$, where the phase angle of which is given by:

$$\text{Ang}(X(1)) = \text{Tan}^{-1}\left(\frac{\text{Im}(X(1))}{\text{Re}(X(1))}\right) \tag{7}$$

where $\text{Im}(X(1))$ and $\text{Re}(X(1))$ are the imaginary and real parts of the complex expression $X(1)$, respectively. The expression in Eq. (10) gives the phase angle of the fundamental frequency with respect to an internal time reference in the IED. It is important to mention here that the time reference from which the angle is measured is not the cosine signal with the nominal system frequency synchronized to the universal coordinated time (UTC) reference as in the case of PMU synchrophasor technique. It is rather an internal time reference in the IED related to the start of sampling process, which is not of significant importance to know since the proposed approach relies on the change in the angle not on the absolute angle value. Assuming the initial phase angle value with respect to the internal time reference is $\theta$, then the phase angle value computed every sinusoidal cycle with respect to that time reference is always $\theta$ if the signal frequency remains at its nominal value. During the acceleration or deceleration of the generator's rotor, the frequency will continuously drift from its nominal value and the phase angle relative to the time reference will keep changing from $\theta$ and the voltage waveform will not be a pure sinusoid. Since the DFT samples the voltage waveform at integer multiples of the nominal or fundamental frequency (in our case, the integer is equal to one), the phasor extraction will not be at the true waveform fundamental frequency and the leakage phenomenon will occur. Leakage is defined as the phenomenon where the energy of the signal spectrum decreases at fundamental and spills over to the higher harmonics. Nevertheless, when the frequency drift is small enough relative to the fundamental frequency value, the leakage will be minimal. If we assume that $\Delta\Phi_i(t)$ defined in Eq. (1) for a slowly continuous varying frequency sinusoid is measured periodically at $t_0$ ms intervals, then it can be proven that these measured phase values

are approximately equal to the phase values of the fundamental component computed by the DFT for that waveform at the same $t_0$ ms intervals [36]. This could be expressed as:

$$\Delta\emptyset|_{t=\theta+nt_0} \cong \Delta\emptyset_{d\_\text{fund},\, t=\theta+nt_0} \tag{8}$$

where $\theta$ is the initial phase angle and $nt_0$ is multiple integer of the sinusoidal cycle time $t_0$. We can recall from Eq. (7) that the discrete phase angle relative to the IED internal time reference and computed at the fundamental frequency by DFT every sinusoidal cycle is calculated as:

$$\Delta\emptyset_{d\_\text{fund},\, t=\theta+nt_0} = \text{Tan}^{-1}\left(\frac{\text{Im}(X(1))}{\text{Re}(X(1))}\right) \tag{9}$$

where $X(1)$ is evaluated at $\theta + nt_0$ intervals. Therefore, the change in discrete angle with time can be used to indicate the change in the generator bus voltage angle and consequently the change in rotor angle $\delta$. Thus, the change in $\Delta\emptyset_{d\_\text{fund},\, t=\theta+nt_0}$ can be used for the angle stability assessment. For simplicity, $\Delta\emptyset_{d\_\text{fund},\, t=\theta+nt_0}$ will be referred to as $\Delta\Phi_d$ in this context. Now, Eq. (5) can be rewritten as:

$$\frac{d\Delta\emptyset_d}{dt} = \frac{d\Delta\delta}{dt} \tag{10}$$

where $\Delta\Phi_d$ is the discrete fundamental phase angle estimated every$t_0$ interval.

### 2.4 Mapping the phase transitions to packet network protocol variables (Network keying)

In principle, the phase angle of the generator bus voltage is computed by the measuring IED or PMU every cycle. In contrary to PMU-based wide area detection schemes, this approach does not necessitate synchronizing all phase measurements over the entire grid and send these measurements by the PMUs continuously in digital streams whether there is a swing or not. It would rather rely on measuring the angle asynchronously by each measuring IED and then transmitting a coded form (or network keyed packets) of the phase angle change asynchronously using a high-speed packet switched network protocol. The transmission will not be continuous, and it shall start only when the phase angle increases beyond a predefined limit. To achieve this, a convenient protocol should be selected. A multicast network protocol would be the best choice here in order to ensure the delivery of multi-source information at any desired destination node simultaneously within a very short transmission time.

The instantaneous phase $\Delta\Phi_i(t)$ will be compared to predefined angle boundaries (from $\beta_1$ to $\beta_n$) as shown in Fig. 4, and the comparison result will be mapped to Boolean variables. However, due to the numerical nature of the IED, it

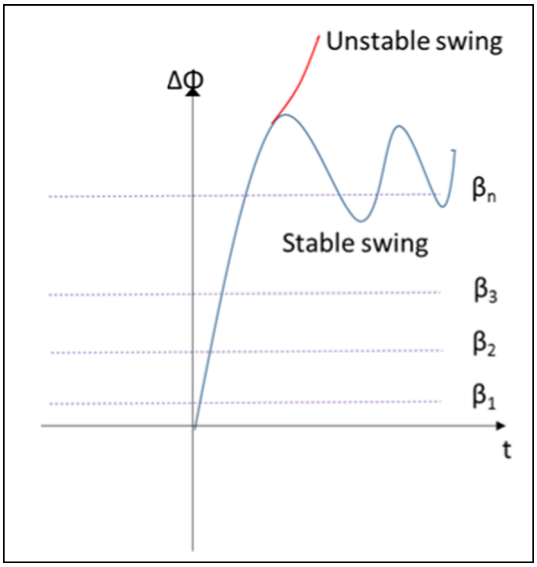


**Fig. 4** Discretization of the phase angle to levels from β1 through βn prior to mapping to Boolean variables

is not able to compute the continuous phase angle $\Delta\Phi_i(t)$ and it will compute instead the discrete $\Delta\Phi_d$ using the DFT. Let$k_1$ through $k_n$ denote Boolean variables of some dataset $D$, $D = \{k_1, k_2, \ldots, k_n\}$. To realize the mapping to Boolean variables, the following conditions shall apply:

$$k_1 = 0 \text{ for } \Delta\Phi_d < \beta_1 \text{while, } k_1 = 1 \text{ for } \Delta\Phi_d \geq \beta_1 \tag{11}$$

$$k_2 = 0 \text{ for } \Delta\Phi_d < \beta_2 \text{while, } k_2 = 1 \text{ for } \Delta\Phi_d \geq \beta_2 \tag{12}$$

$$k_n = 0 \text{ for } \Delta\Phi_d < \beta_n \text{while, } k_n = 1 \text{ for } \Delta\Phi_d \geq \beta_n \tag{13}$$

where $\beta_n$ is the farthest phase boundary corresponding to some phase value below 180 degrees. The Boolean variables will then be transmitted sequentially in packets using the multicast protocol. To have an insight on the transmitted packets content, the acceleration cycle of power swing will be considered as an example. As the rotor accelerates, $\Delta\Phi_d$ will keep increasing; thus, the k Boolean variables will be incrementing from 0 to 1 sequentially. Then, the expected pattern of the Boolean sequence streams transmitted on the network will be as follows:

Sequence $1 = \{1,\ 0,\ 0 \ldots .. \ldots 0,\ 0\}$

Sequence $2 = \{1,\ 1,\ 0 \ldots .. \ldots 0,\ 0\}$

Sequence $m = \{1,\ 1,\ 1,\ ..1,\ ..,\ 0,\ 0\}$

where $m$ is some integer less than n.

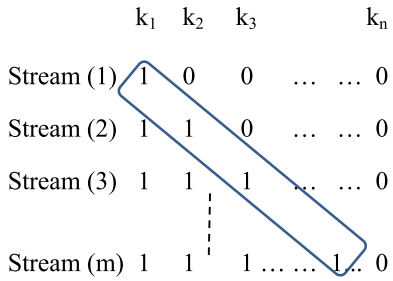


**Fig. 5** Fast monotonic swing as indicated by the all ones diagonal of the matrix

The transmitted Boolean sequences during acceleration can be expressed in matrix form as:

The stream m above exhibits the peak of the monotonic change of the variable $\Delta\delta$ with time during the acceleration cycle of power swing. The successive increment of the values of Boolean variables can also be noticed from one stream to the stream following it as shown in the diagonal of the matrix of Fig. 5.

## 2.5 Measuring perturbation in power grid using the GOOSE protocol

In this section, we will demonstrate how the sought protocol to fulfill the requirements of the approach introduced in the above section is very close to the Generic Object Oriented Substation Event (GOOSE) protocol or its successor Routable GOOSE (R-GOOSE). Yet, the handling of both of them needs to be manipulated to accommodate the dynamics of the electrical grid and its phase angle variations. The following subsection provides a brief introduction of the GOOSE protocol operation.

### 2.5.1 GOOSE protocol operation

Being an extremely fast protocol, the GOOSE is normally used in the transmission of critical signals and events in a power system such as trip commands or protection related signals to guarantee a reliable and fast transmission of signals between IEDs. The IED transmitting the signal of interest will send it over the local area network (LAN) to all IEDs connected to this LAN and hence comes the name multicast protocol. The transmitting device is called the publisher, while the device interested in the transmitted information will subscribe to the network to get it and thus it is called the subscriber.

For the protocol handler in the IED to carry out this function, it defines some important parameters such as [37]:

- Dataset: contains the data attributes to be transmitted through the GOOSE message.

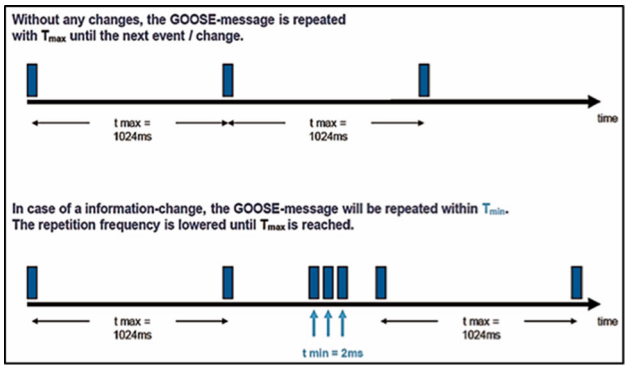


**Fig. 6** GOOSE transmission in steady-state and data change conditions

- State Number: the counter that increments each time a GOOSE message has been sent and a value change has been detected within the dataset.
- Sequence Number: the counter that shall increment each time a GOOSE message has been retransmitted.

Any change in the content of the dataset elements of a GOOSE Control Block is signaled at the receiving end by an increment in the packet state number [37], which in turn invokes the subscribing IED to extract the GOOSE data attributes and write their values in the IED data model. If the state number is unchanged, the IED does not have to pass the GOOSE content to the data model. The sequence number is incremented only if a GOOSE message with the same content is retransmitted at a time, as it should be retransmitted periodically in time according to a predefined rate. At steady state without change in the dataset values, the GOOSE packets are transmitted with their "Max. Time" period which is usually in the range of few seconds in typical IEDs.

If none of the dataset attributes changes for a given time, the packets are retransmitted (with the same dataset attributes). If the dataset attributes remain unchanged, the packets are retransmitted at a continually increasing interval of time starting from the "Min. Time" (which is in the range of few milliseconds) till the "Max. Time" is attained again indicating the new steady-state transmission. These retransmitted packets are known as "heart beats" (Fig. 6).

In a power grid, if a disturbance occurs at an initial rotor phase angle $\delta_0$ of a given generator, then the rotor phase angle will change with time with respect to $\delta_0$. The Boolean variables $k_1$ to $k_n$ defined in Sects. 2.4 and 2.5 will be the elements of the dataset of the GOOSE.

Accordingly, if any of the$k$ variables change as a result of the bus angle change, the GOOSE protocol handler will immediately send a packet and increment its state number by one relative to the last transmitted packet. In this way, any angle change is signaled instantaneously through the LAN to the detecting IED. Therefore, the rate of angle change is

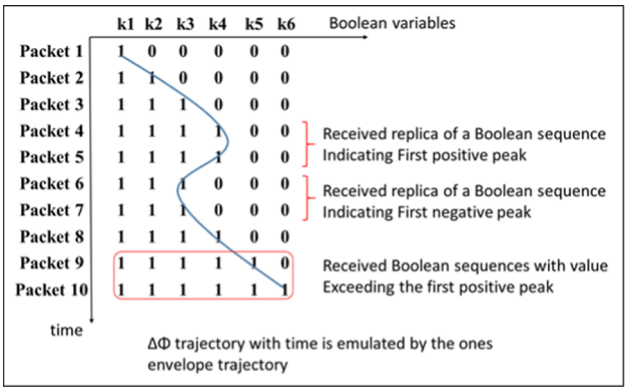


**Fig. 7** Expected received sequence pattern versus time showing one positive peak and one negative peak, indicating non-monotonic quasi-oscillatory unstable swing

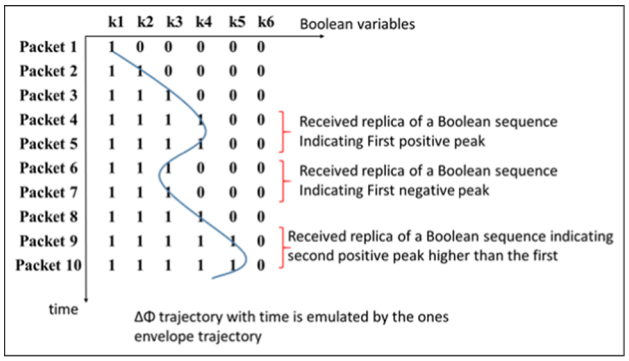


**Fig. 8** Expected received sequence pattern versus time. The second positive peak is higher than the first, indicating non-monotonic oscillatory unstable swing

perceived from the GOOSE packets transmission rate or their state number increment rate.

Using Eq. (10), this rate could be expressed mathematically as:

$$\alpha = \frac{d\Delta\emptyset_d}{dt} = \frac{d\Delta\delta}{dt} \tag{14}$$

where $\alpha$ is the GOOSE packets transmission rate due to angle change.

To understand the proposed scheme, it is worthwhile to consider it as mimicking the rotor angle dynamics in time domain by the transmission pattern of the packets over the data network associated with the power system. The reaction of the detecting device will depend not only on the packets data content but also on their transmission pattern.

Equation (14) reveals that in the case of fast monotonic angle increase, there will be a continuous increment in the Boolean sequence and consequently a continuous published stream of GOOSE packets showing consecutive increment of their state number.

If the angle settles to a constant value, no further packets will be transmitted. This silent period is signaled in the GOOSE protocol by the retransmission of the last packet content with the same state no., but with incrementing sequence no. with each retransmission packet. The GOOSE first retransmission time is set to a value higher than the electrical sinusoidal cycle (20 ms for the 50 Hz system and 16.67 ms for 60 Hz system) or even higher than integer multiples of it to allow for the possible slow change of the variable $\Delta\delta$.

Therefore, in case of slow angle change as in the case of rotor speed approaching its nominal value, GOOSE retransmission packet will appear; consequently, the detecting device will receive a replica of Boolean sequence, indicating a local maximum or positive peak of the angle curve with time as depicted in Fig. 7 in packets 4 and 5. The curve in the figure tracks the Ones envelope in all packets, which mimics $\Delta\Phi_d$ trajectory. If this first peak occurs, we have three possibilities according to [32]:

1. A local minimum or a negative peak occurs after the first positive one, indicated by a replica of sequence that is decremented in its Ones content with respect to the first peak. If the Boolean sequences subsequent to the negative peak increment consecutively till they exceed the first positive peak, this will indicate an unstable swing. Figure 7 shows GOOSE packets 9 and 10 with consecutively incremented One Boolean content. This case is quasi-oscillatory case in this literature to distinguish it from other cases. This case corresponds to non-monotonic unstable swing where the generator rotor starts to accelerate again indefinitely after a temporary deceleration cycle.
2. A second positive peak higher than the first one occurs, indicated by a replica with incremented Ones with respect to the first replica, which will indicate unstable oscillation. Figure 8 shows the three peaks indicated by the packet pairs (4)–(5), (6)–(7) and (9)–(10), respectively.
3. A second positive peak lower than the first one occurs, indicated by a replica with decremented ones with respect to the first replica, which will indicate stable oscillation. Figure 9 shows the three peaks indicated by the packet pairs (5)–(6), (8)–(9) and (10)–(11), respectively.

It can be noticed that the above first and second unstable cases (shown in Figs. 7 and 8, respectively) trigger similar GOOSE response since the instability in both could be indicated by the appearance of packet (9) sequence whose Ones' content is exceeding that of the first peak. Accordingly, in this work, the unstable case will be indicated by the moment of increasing ones in the Boolean sequences relative to the first positive peak whether the angle trajectory is oscillating or not.

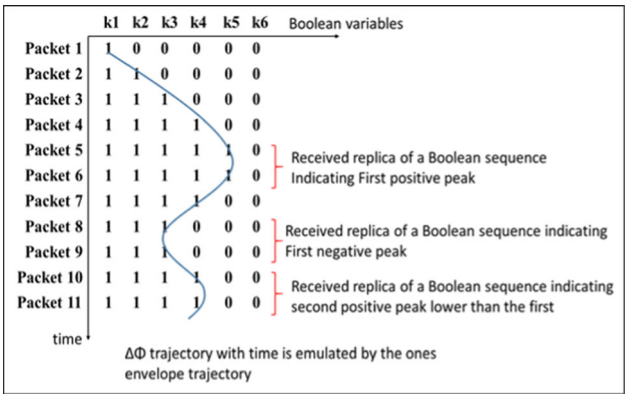


**Fig. 9** Expected received sequence pattern versus time. The second positive peak is lower than the first indicating oscillatory stable swing

Based on the above argument, we are now left with three cases of stability, namely the monotonic unstable case, the stable oscillating case and the non-monotonic unstable case. The last case comprises oscillatory and quasi-oscillatory cases.

It is important to mention here that the above argument for GOOSE protocol is valid for R-GOOSE protocol since their behavior is the same. The only difference is that R-GOOSE uses UDP/IP protocol for routing over wide area network, while GOOSE uses the media access control (MAC) address for communication over LAN or extended LAN, i.e., LAN is extended to other remote devices using point-to-point transmission equipment; thus, MAC addresses are used for communications over extended LAN without IP routing. It is also important to recall here the fact that the data transfer time for both protocols is as low as 3 ms from the publisher to subscriber devices for critical protection signals [38, 39].

Thus, the data transfer between the measuring and detecting devices in the proposed scheme is almost real time.

## 3 Simulation results and discussion

In this section, three parts of simulations are conducted, the first part aims to demonstrate the concept of the induced GOOSE in response to phase angle change as in the case of an oscillating generator, the second part is a realization of real GOOSE transmission from a simulated IED on real network in the case of monotonic unstable power swing, and the third part is a case study of simulated disturbance on IEEE 39-bus system to test the response of the proposed scheme to stable and unstable swings. Discussions on the results are presented in the end of the section.

### 3.1 GOOSE Transmission from a simulated IED during monotonic unstable swing over a real network

The simulator used in this part is IEC 61850 Xelas Energy Management. The simulator will be used to emulate a real IED measurement device. The Wireshark network analyzer will be used for the packets display and analysis. The Substation Configuration Language (SCL) file (refer to Appendix 1) imported in the simulator is a typical file of a P442 distance protection relay manufactured by GE.

The SCL file defines the basic IEC 61850 parameters such as the logical device, logical nodes and data objects of the protection and measurements functions of the physical device. It defines also the communication service blocks such as report control blocks and GOOSE control blocks where the dataset of the Boolean variables used in this scheme is located.

The distance protection function is usually used in the generator protection to detect power swing and hence enables the generator protection to discriminate between actual fault and swing. In addition, it discriminates between stable and unstable swing based on the classical impedance measurement method as mentioned in the introduction of this paper. Nevertheless, the power swing function in the simulated relay will not be used and the estimated voltage phasor angle will be used instead to implement the proposed scheme. Figure 10 shows the setup deployed in the simulation.

The SCL file is imported to Xelas simulator on two PCs as shown in Fig. 10. The below data attribute of the relay IEC 61850 model is used as the generation bus voltage angle:

*EWL03_P442Measurements/SecFouMMXU1.PhV.MX .phsA.cVal.ang.f*

Appendix 1 helps the reader to recognize the simulator view and the structure of an IEC 61850 data object

The data attribute mentioned above, which represents $\Delta\Phi_d$ of the generator bus voltage, is increased using the simulator in a continuous manner similar to the case of fast unstable swing.

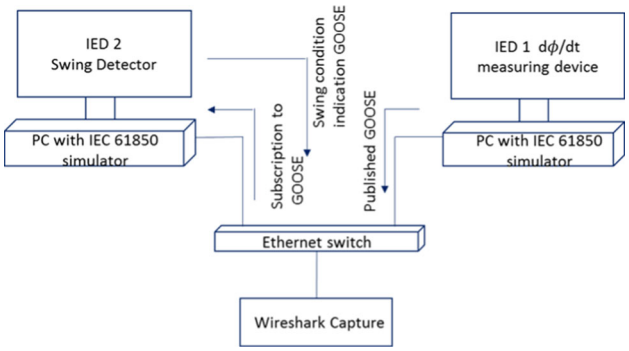


**Fig. 10** Simulation setup

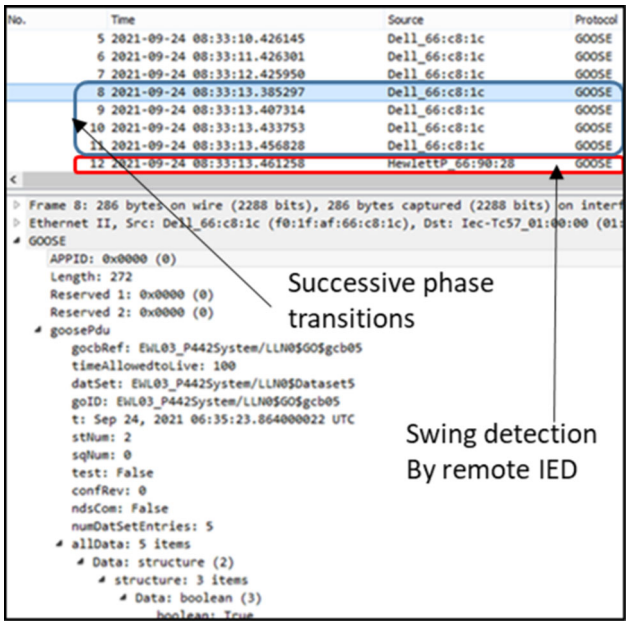


**Fig. 11** Wireshark capture showing the GOOSE packets published by the measuring IED (packets 8 through 11). Packet 12 is the response packet from the detecting IED

The mapping is accomplished by entering Eqs. (11) through (13) with $n = 4$ as preconditions in the simulator for 30-degree-angle steps from 0 to 120 degrees. The angle is changed at a rate of 30 degrees every 20 ms approximately. As a result, the Boolean variables from $k_1$ to $k_4$ change from 0 to 1 successively. This will invoke the transmission of four GOOSE packets successively from the measuring device IED 1.

The Wireshark capture in Fig. 11 shows the four GOOSE packets numbered from 8 through 11 published by the measuring IED and the packet 12 which is the response from the detecting IED (IED 2 according to Fig. 10) after detecting the fast swing. The content of packet 8 is displayed in the bottom pane of Fig. 11.

Figure 12 shows graphical representation of the five consecutive packets with time. The GOOSE packets are shown as pulses, where the pulse is dark shaded when the corresponding $k$ variable is equal to one and it is not shaded when the $k$ variable is equal to zero.

This simulation represents a hypothetical case of a very fast unstable swing and hence demonstrates the capability of the proposed scheme to detect the worst real fast swings which are certainly slower that this hypothetical case. The Boolean sequence content of the four packets is depicted in Fig. 12. The $k$ Boolean sequences are (1000), (1100), (1110) and (1111), corresponding to the angle changes of 30, 60, 90 and 120 degrees, respectively.

Therefore, the Boolean sequences increment consecutively without replica or retransmission packet between

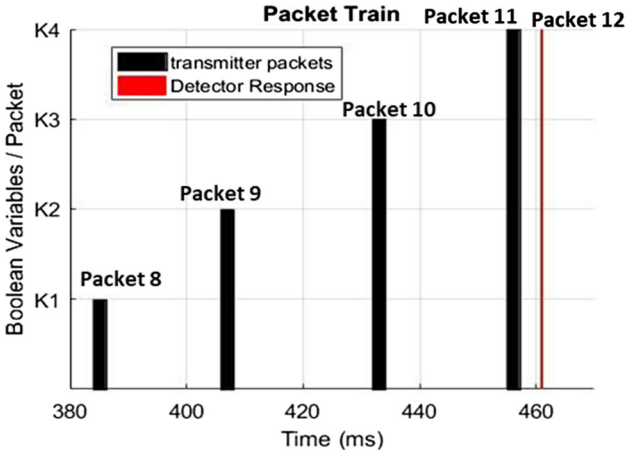


**Fig. 12** Published GOOSE packets versus time

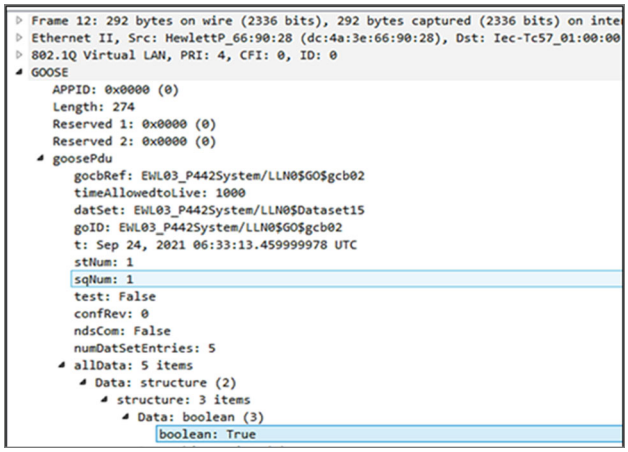


**Fig. 13** Wireshark capture of the response packet 12. The detection of fast swing is indicated by the Boolean true

them, indicating monotonic fast swing. The remote detecting device IED 2 responds to the successive change of the Boolean variables and hence to monotonic rotor angle increase by packet 12 as shown in Fig. 11. Thus, this packet indicates unstable swing detection. According to [40], 120 degrees is the critical angle shift defined as the criteria to decide the instability condition. However, this is a conservative limit and it can be further increased for more precise assessment of stability. This will be realized in Sect. 3.2 of simulation and results.

It is observed from the timestamps of the recorded packets in Fig. 12 that the detection packet 12 takes place after the packet corresponding to the critical angle change (packet 11) by 5 ms approximately. The content of packet 12 is displayed in Fig. 13.

It is worth to note here that the 5-ms time interval is the average processing time of the scheme based on real packet network, obtained after conducting many simulations. Hence, it can be considered as the scheme average response

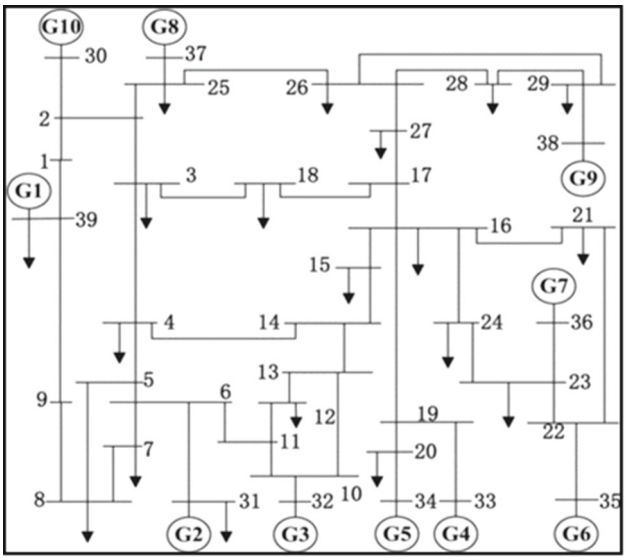


**Fig. 14** IEEE 10-machine 39-bus system

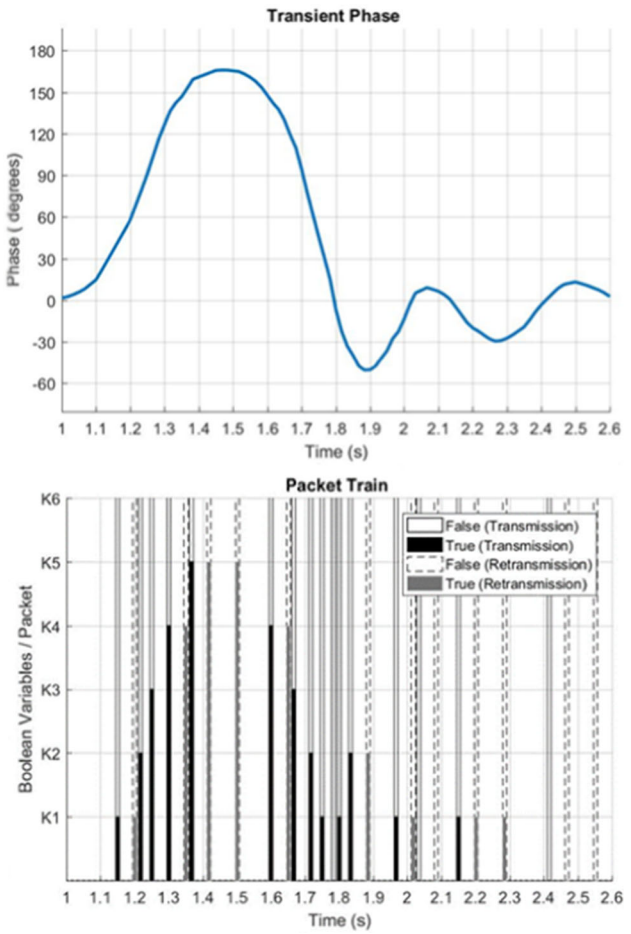


**Fig. 15** **a** Rotor angle variations in the case of stable swing and **b** the equivalent induced GOOSE packets with Boolean variables

time to monotonic change over any IEC 61850-based network. It is also independent on the number of phase boundary levels ($\beta_1$ to $\beta_n$) or critical angle. The network behavior of the stable oscillating swing case is also simulated in this work in Sect. 3.2.

### 3.2 Response of the proposed scheme to a simulated disturbance in New England 10-machine 39-bus system

The results of a simulated disturbance in the IEEE 10-machine 39-bus system obtained as per [32] for both stable and unstable cases are used to test the response of the proposed scheme. New England 39-bus system is a 60 Hz, 10-generator system with slack generator G2 at bus 31. Figure 14 depicts the IEEE 39-bus system. According to [32], a stable disturbance is simulated by creating a three-phase-ground fault at bus 2 at 1 s. Then, the fault is cleared by tripping the line 2–3 at the time instant 11.33 s. Figure 15a shows the relative angle of the most disturbed generator pair (MDGP) according to [32], which can be considered—in a reasonable approximation—as the worst-case phase deviation for a disturbed generator relative to the grid in the proposed scheme. The angle values of the shown simulation curve in Fig. 15a are entered to MATLAB. Six $\beta$ boundaries are taken uniformly spaced by 30 degrees with corresponding six $k$ variables.

The simulated GOOSE train as published by the measuring IED corresponding to the angle variations is shown as rectangular pulses. The dark part of each pulse corresponds to the Boolean variables with True or One values.

It can be obviously seen from Fig. 15 that the positive and negative peaks exhibit silent periods without new GOOSE transmission. These silent periods are interrupted by one or more replica (or retransmission) packet shown as a dashed pulse in the figure, the shaded part of which corresponds to the Boolean variables with True or One values. The GOOSE retransmission time is taken as three sinusoidal cycles (50 ms). It can also be noticed that each peak is indicated by a replica or a retransmission packet followed by a packet with decremented or incremented Boolean sequence relative to that of the retransmission.

It can be seen from Fig. 15 that there is one retransmission packet at 1.35 s before the angle reaches 150 degrees with Boolean sequence (111100), which indicates that the phase change rate starts to decrease and therefore the Boolean content of the subsequent packets shall be investigated. The packet next to the first retransmission shows an incremented Boolean sequence of (111110); however, this packet is followed by two retransmission packets at 1.433 s and 1.5 s, and then, the packet at 1.6 s shows a decremented sequence of (111100), which indicates the first positive peak in the oscillatory pattern. Similarly, there is a subsequent negative peak indicated by retransmission packet at 1.88 s with Boolean sequence (110000) followed by a packet at 1.96 s

with decremented Boolean sequence (100000). It should be noted here that the mapping rules in the positive $\beta$ angle ranges mentioned in Eqs. (11) through (13) are symmetrical to the mapping rules in the negative $\beta$ angle ranges. Thus, for the range of phase angle between 0 and $-30$ degrees, the $k_1$ variable is set equal to 1 and for angle between $-30$ and $-60$, $k_2$ is set equal to 1. Thus, the Boolean contents of the packets published at 1.82, 1.88 and 1.96 s reveal negative angle values where the angle at 1.96 is greater than that at 1.88 s. The second positive peak is indicated by the retransmission packet at 2.08 s with sequence (000000) followed by a packet at 2.15 s with an incremented sequence (100000). It is to be noted here also that at 2.15 s the angle goes below zero and the mapping rules imply that $k_1$ becomes one after being zero at 2.08; thus, the sequence (100000) actually reveals that the angle value becomes negative after the positive value attained at this peak.

From the above argument, it can be concluded that there are two positive peaks with a negative peak in between. The Boolean sequence corresponding to the first positive peak contains larger number of ones than that of the second positive peak. This indicates a stable swing according to Case (3) shown in Fig. 9 in Sect. 2.5, Accordingly, the decision of stable swing will be declared shortly by the detecting IED after the packet published by the measuring IED at 2.15 s is received. This declaration period is calculated from a simulation of a similar swing with the same oscillatory behavior using the simulation setup shown in Fig. 14 using Xelas IEC 61850 tool. In this simulation, the data attribute $\Delta\Phi_d$, *EWL03_P442Measurements/SecFouMMXU1.PhV.MX .phsA.cVal.ang.f* defined in Sect. 3.1, is set to follow a similar angle behavior shown in Fig. 15a. The detecting IED subscribes to the published GOOSE packets and detects the oscillatory stable swing accordingly.

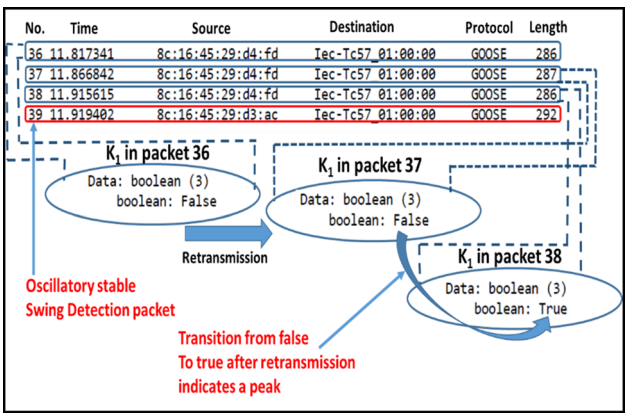


**Fig. 16** Rotor angle variations in the case of oscillatory stable swing. Packets 36, 37 and 38 are expanded to show the value of $k_1$ variable. Packet (39) indicates oscillatory stable swing

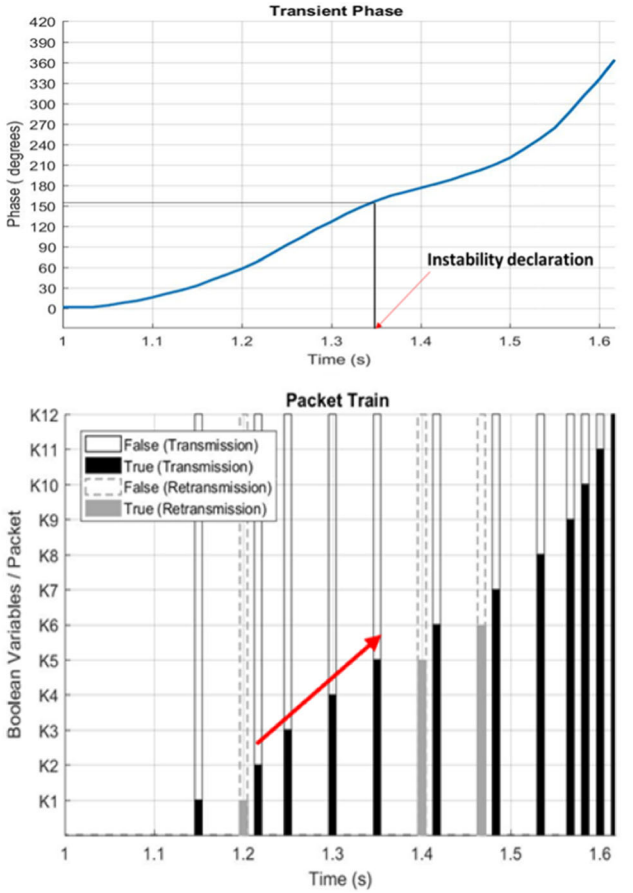


**Fig. 17** **a** Rotor angle variations in the case of unstable swing and **b** the induced GOOSE. The monotonic increment of Boolean variables in the GOOSE packets is indicated by red arrow

Figure 16 shows the Wireshark capture obtained from the simulation of the oscillatory stable case. We will focus the capture on the induced packets around the second positive peak of the angle curve. The false value of the variable $k_1$ in packet 36 is retransmitted in packet 37, and then, $k_1$ turns to true in packet 38. This corresponds to the retransmission of the sequence (000000) and then its transition to sequence (100000) as typically shown in Fig. 15b. This indicates the second positive peak. Packet 38 in Fig. 16 corresponds to the packet at $t = 2.15$ s in Fig. 15. Packet 39 in Fig. 16 sent by the detecting IED indicates the detection of stability. As it can be seen, the difference in timestamp between packets 38 and 39 in Fig. 16 is 4 ms; therefore, it can be deduced that the stability declaration time would be at 2.154 s.

The unstable case is simulated according to [32] by increasing the fault clearing time to 1.331 s instead of 1.33. G1 is the most disturbed generator in this case. It is observed that the angle grows until it is out of step (passing 180 degrees indicates instability). Figure 17 depicts the unstable case.

It can be seen from Fig. 17 that there is an inrush of GOOSE frames starting from a phase angle change value of

60 degrees till 150 degrees without ceasing (without retransmission or replica packet), which indicates that most likely the angle will not recover before 180-degree limit and the generator will lose synchronism.

According to the second simulation part in Sect. 3.2, the instability is declared 5 ms later to the packet corresponding to the critical rotor angle change. This packet appears at 1.35 s and corresponds to a critical change of angle equal to 150 degrees. Thus, the instability is declared at 1.355 s. The value of 150 degrees is chosen here as the critical angle shift rather than the 120-degree limit defined in [40] to allow for more precise monitoring of rotor angle before final judgment of instability; meanwhile, there is still enough time to take a control action.

Comparing this with the results of [32], the prediction of rotor angle instability based on auto-regression (AR) scheme is declared at 1.333 s. However, according to MLE, the instability is declared at 1.6 s, although the generator has already been unstable since the time instant 1.467 s. Therefore, the MLE method failed to predict the instability condition before its actual occurrence, while both the proposed scheme and the AR technique of [32] succeed to predict the instability before its occurrence by 112 and 134 ms, respectively.

It is worth to mention here that although the proposed scheme response is slightly slower than the AR PMU-based scheme, there would be enough time to take the appropriate control action in both schemes before the affected generator loses stability. In addition, it is possible to decrease the needed prediction time by increasing the number of $\beta$ levels; thus, the permissible angle shift can be reduced slightly below 150 degrees.

In summary, we have conducted several simulations in this section to prove the effectiveness of the scheme. First, the concept of induced GOOSE packets in response to changes in rotor phase angle is demonstrated. Then, a real IEC 61850 network has been constructed, where the induced packets are used to identify instability. The average measured detection time is found to be 5 ms in the fast monotonic swing case and 4 ms in the oscillatory stable case. Finally, the scheme was used to detect the swing of the affected generators due to a simulated disturbance in the IEEE 39-bus system. The results show that the scheme can discriminate between both stable and unstable swings; in addition, it predicts the fast unstable swing of the affected generator ahead of its occurrence by 112 ms approximately.

### 3.3 Discussion

Since the proposed scheme proves an efficient way for stability assessment while using existing IEDs only without adding PMUs, it can lend itself to actually implemented WAM systems. As an example of the existing WAMS systems that has been studied to be upgraded to be a real wide area monitoring, protection and control (WAMPAC) system is that of the Croatian 400 and 220 kV network. The system described in [42] proposes using voltage angle difference between two buses ($\Delta\Phi$) to establish a criterion for stability assessment. The criterion to initiate out-of-step protection (OOS) tripping has been set as $\Delta\Phi \geq 20$ degrees. $\Delta\Phi$ is measured as the phase angle between two network sections, where each section is provided with a PMU connected to one of its buses. In this regard, the scheme we propose in this paper can be deployed in the proposed WAMPAC system of [42] to replace the PMU function of computing the bus voltage angle with the same function inherent in one of the already existing protection relays. This relay can be that the connected to the section bus or to the transmission line connected to it, such as the distance protection relay or the line differential relay. Only One relay on either side shall be used to compute its bus voltage angle and transmit the induced GOOSE packets in direct proportionality to the rate of change of the angle in the case of swing in the way described above. Since the system used in [42] is modeled by a two-source equivalent model, the change in the measured bus angle here can be essentially referred to the other section bus. One detector device shall be located in the Control Center to detect the induced GOOSE packets and apply the criterion of successive increment of GOOSE sequence without retransmission in between as described in Sect. 3.2 to detect unstable swing. This detector function can be either integrated in the WAMPAC system or provided as standalone device capable pf communication with the WAMPC.

In addition to saving the costs of PMUs and avoiding complexity of processing, the time performance of the proposed non-PMU-based approach can be much better than that of the PMU-based one. The total processing time of the unstable or OOS swing using the non-PMU-based scheme is about 5 ms compared with the reported values in [42] of about 20-ms transmission delay in addition to processing delay less than 100 ms.

## 4 Conclusion

In this paper, a new wide area network scheme is developed for power swing detection based on deploying the intrinsic characteristics of GOOSE or R-GOOSE multicast protocols. Unlike the common approach in the existing WAMS schemes of applying diverse mathematical algorithms of grid stability assessment, the new scheme introduces a method to standardize the stability assessment process. The scheme adopts

the estimation of the rate of change of the angle of the generator bus voltage as computed by the IED connected to the generator bus, which has been proven to be the same as the rate of change of the generator rotor angle. The calculated bus voltage angle is mapped to Boolean variables that are in turn transmitted via the multicast protocol. It has been proven that the pattern of the data packets transmitted on the network via the GOOSE/R-GOOSE protocol mimics the swing pattern on the electrical power grid; therefore, the packets' transmission pattern can be used to assess the stability of the grid. A wide area network communication scheme has advantages over existing offline traditional methods that it does not require extensive offline studies of the power systems and does not require network reduction for multi-machine power systems. Moreover, it has advantages over other available WAMS schemes that it does not need additional GPS-synchronized measuring device like PMU. Also, it does not require continuous transmission of measured angle and angular speed values. The effectiveness of the proposed method is tested by simulating disturbances on the IEEE 39-bus system for both stable and unstable cases. The results show that the scheme can discriminate between stable and unstable swings. In the case of fast monotonic unstable swing, the loss of synchronism of the affected generator is predicted ahead of its occurrence by more than 100 ms, which gives enough time to take an appropriate control action.

**Author's contributions** EAEM wrote the main manuscript text. MAA and MES reviewed the figures and results. All authors reviewed the final manuscript.

**Funding** Open access funding provided by The Science, Technology & Innovation Funding Authority (STDF) in cooperation with The Egyptian Knowledge Bank (EKB).

**Availability of data and materials** The authors declare that any required data can be made available upon request.

## Declarations

**Conflict of interest** The authors hereby declare that they have no competing interests as defined by Springer or other interests that might be perceived to influence the results and/or discussion reported in this paper.

**Ethical approval** Not applicable.



## Appendix (1)

### IEC 61850 data object name structure

IEC 61850–6 defines the SCL file of an IED or a group of IEDs. The SCL is an XML written file that contains a set of definitions related to the IED hardware, manufacturer and device functions modeled as logical device, logical nodes and data attributes. The SCL file contains as well communication configuration data such as the IP address and subnet mask of the device in the network. The datasets including the data attributes describing the device functions are also included in the file. These datasets are the container that can be transmitted via communication protocols such as GOOSE from the IED to other devices connected to the same network.

According to IEC 61850 standard, the data object name is defined as per the syntax in Fig. 18.

For the following IEC 61850 data attribute: ***EWL03_P442Measurements/SecFouMMXU1.PhV.MX.phsA.cVal.ang.f***, the data anatomy is as follows:

***EWL03_P442*** is the physical measuring device, ***EWL03_P442Measurements*** is the logical device with measurement function.

***SecFouMMXU1*** has two components. *SecFou* is a prefix for Fourier transform of the secondary winding measurement of the voltage transformer. The second component is the MMXU1 which is the logical node of the voltage measurement. ***PhV.MX.phsA.cVal.ang.f*** is the phase angle of the phase to ground voltage phasor of Phase A, computed every cycle of the sinusoidal waveform.

The above data attribute represents the phase angle value ($\Delta \Phi_d$) of the generator bus voltage phasor relative to a time reference in the IED. This value is calculated by the IED by

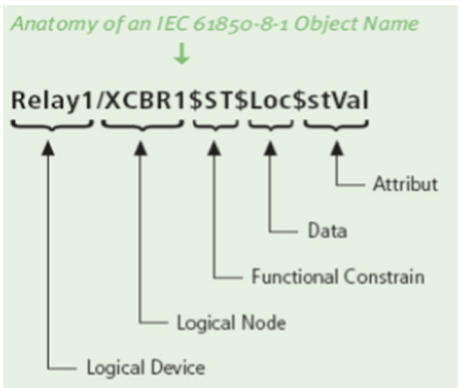


**Fig. 18** Example of data object name as defined in IEC61850 standard

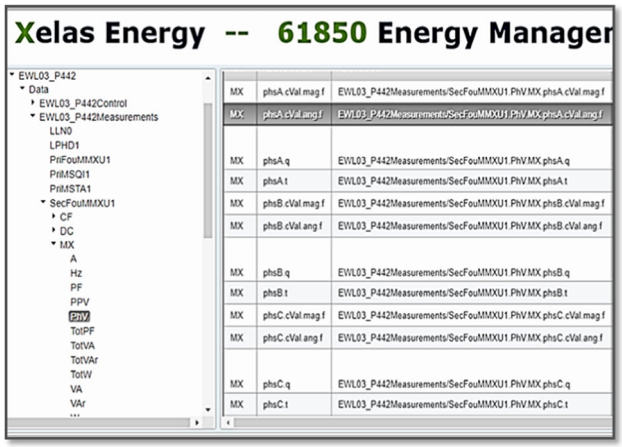


**Fig. 19** Snapshot of the Xelas IEC 61850 simulator showing the data object of generator bus voltage angle

applying DFT to the sampled voltage signal at the fundamental frequency.

In this paper, the above-mentioned data attribute is mapped to Boolean variables which constitute a dataset. This dataset is then transmitted via GOOSE protocol to the detecting device. The Boolean variables in this work are taken as data objects of a generic input/output logical node (GGIO) defined in the relay SCL file.

Figure 19 shows a screen view of the simulator which displays the above IEC 61850 data attribute of the said relay [41].

## References


1. Yellajosula JRAK, Wei Y, Grebla M, Paudyal S, Mork BA (2020) Online detection of power swing using approximate stability boundaries. IEEE Trans Power Delivery 35(3):1220–1229. https://doi.org/10.1109/TPWRD.2019.2941522
2. Fischer N, Benmouyal G, Hou D (2012) Tutorial on power swing blocking and out-of-step tripping. In: 39th Annual Western protective relay conference Spokane, Washington October 16–18, 2012.
3. IEEE Power System Relaying Committee Working Group D6, "Power swing and out-of-step considerations on transmission lines (2006).
4. Elmore WA (2004) Protective relaying theory and applications, 2nd edn. Marcel Dekker, New York
5. Taylor CW, Haner JM, Hill LA, Mittelstadt WA, Cresap RL (1983) A new out-of-step relay with rate of change of apparent resistance augmentation. In: IEEE transactions on power apparatus and systems, vol. PAS-102, no. 3, pp. 631–639. https://doi.org/10.1109/TPAS.1983.317984.
6. Tziouvaras DA, Hou D (2004) Out-of-step protection fundamentals and advancements. In: Proceedings of 57th annual conference for protective relay engineers, pp 282–307.
7. Fischer N, Benmouyal G, Hou D, Tziouvaras D, Finley JB, Smyth B (2012) Do system impedances really affect power swings—applying power swing protection elements without complex system studies. In: Proceedings of 65th annual conference for protective relay engineers, Apr. 2012, pp 108–119.
8. Zhang S, Zhang Y (2017) A novel out-of-step splitting protection based on the wide area information. IEEE Trans Smart Grid 8(1):41–51
9. Padiyar KR, Krishna S (2006) Online detection of loss of synchronism using energy function criterion. IEEE Trans Power Delivery 21(1):46–55
10. Holbach J (2003) New blocking algorithm for detecting fast power swing frequencies. In: Proceedings of the 30th annual western protective relay conference, Spokane, WA, October 2003.
11. Mohammadi A, Abedini M, Davarpanah M (2021) A straightforward power swing detection algorithm using rate of impedance angle change. IEEE Trans Power Deliv. https://doi.org/10.1109/TPWRD.2021.3127451.
12. Salehimehr S, Taheri B, Faghihlou M (2022) Detection of power swing and blocking the distance relay using the variance calculation of the current sampled data. Electr Eng 104:913–927. https://doi.org/10.1007/s00202-021-01350-1.
13. Rebizant W, Feser K (2001) Fuzzy logic application to out-of-step protection of generators," 2001 Power Engineering Society Summer Meeting. In: Conference proceedings (Cat. No.01CH37262), 2001, pp. 927–932 vol 2. https://doi.org/10.1109/PESS.2001.970179.
14. Abdelaziz AY, Irving MR, Mansour MM, El-Arabaty AM, Nosseir AI (1998) Adaptive protection strategies for detecting power system out-of-step conditions using neural networks. IEE Proc Generation Trans Distrib 145(4):387–394
15. Hashiesh F, Mostafa HE, Helal I, Mansour MM (2010) A wide area synchrophasor based ANN transient stability predictor for the Egyptian Power System. IEEE PES Innovative Smart Grid Technologies Conference Europe (ISGT Europe) 2010, pp 1–7. https://doi.org/10.1109/ISGTEUROPE.2010.5638923
16. Amraee T, Ranjbar S (2013) Transient instability prediction using decision tree technique. IEEE Trans Power Syst 28(3):3028–3037. https://doi.org/10.1109/TPWRS.2013.2238684
17. Kundu P, Pradhan A (2014) Wide area measurement based protection support during power swing. Int J Electr Power Energy Syst 63(4):546–554
18. Rajapakse AD, Gomez F, Nanayakkara K, Crossley PA, Terzija VV (2010) Rotor angle instability prediction using post-disturbance voltage trajectories. IEEE Trans Power Syst 25(2):947–956
19. Mahmoud RA, Malik O (2022) Out-of-step detection of synchronous generators using dual computational techniques based on correlation and instantaneous powers. IET Generation Transm Distrib. https://doi.org/10.1049/gtd2.12485, 16,13 (2716–746)
20. Hosseini SA, Taheri B, Abyaneh HA et al (2021) Comprehensive power swing detection by current signal modeling and prediction using the GMDH method. Prot Control Mod Power Syst 6:15. https://doi.org/10.1186/s41601-021-00193-z
21. Centeno V, Phadke AG, Edris A, Benton J, Gaudi M, Michel G (1997) An adaptive out-of-step relay [for power system protection]. IEEE Trans Power Delivery 12(1):61–71
22. Paudyal S, Ramakrishna G, Sachdev MS (2010) Application of equal area criterion conditions in the time domain for out-of-step protection. IEEE Trans Power Delivery 25(2):600–609
23. Paudyal S, Gokaraju R, Sachdev MS, Cheng S (2009) Out-of-step detection using energy equilibrium criterion in time domain. Electric Power Compon Syst 37(7):714–739
24. Paudyal S, Ramakrishna G, Sachdev MS (2008) Out-of-step protection using the equal area criterion in time domain—smib and 3-machine case studies. In: Proceedings of IEEE Region 10 Conference (TENCON), Nov 2008, pp. 1–6.
25. Paudyal S, Gokaraju R (2015) Out-of-step protection for multimachine power systems using local measurements. IEEE Eindhoven PowerTech 2015:1–6. https://doi.org/10.1109/PTC.2015.7232481

26. Xue Y, Custem TV, Ribbens-Pavella M (1989) Extended equal area criterion justifications, generalizations, applications. IEEE Trans Power Syst 4(1):44–52
27. Pai MA (1981) Power system stability: analysis by the direct method of Lyapunov. North-Holland Publishing Company, Amsterdam
28. Kundur P (1994) Power system stability and control. McGraw-Hill, New York
29. Farantatos E, Huang R, Cokkinides GJ, Meliopoulos AP (2016) A predictive generator out-of-step protection and transient stability monitoring scheme enabled by a distributed dynamic state estimator. IEEE Trans Power Delivery 31(4):1826–1835
30. Yu YN, Vongsuriya K (1967) Nonlinear power system stability study by Liapunov function and Zubov's method. In: in IEEE transactions on power apparatus and systems, vol. PAS-86, no. 12, pp. 1480–1485.
31. Wei S, Yang M, Qi J, Wang J, Ma S, Han X (2018) Model-free MLE estimation for online rotor angle stability assessment with PMU data. IEEE Trans Power Syst 33(3):2463–2476. https://doi.org/10.1109/TPWRS.2017.2761598
32. Chandraa A, Pradhanb AK (2020) Model-free angle stability assessment using wide area measurements. Int J Electr Power Energy Syst 120:105972
33. Wang S, Yu J, Zhang W (2019) Transient stability assessment using individual machine equal area criterion part III: reference machine. IEEE Access 7:80174–80193. https://doi.org/10.1109/ACCESS.2019.2921035
34. Wang B, Fang B, Wang Y, Liu H, Liu Y (2016) Power system transient stability assessment based on big data and the core vector machine. IEEE Trans Smart Grid 7(5):2561–2570. https://doi.org/10.1109/TSG.2016.2549063
35. Ren C, Xu Y (2022) Robustness verification for machine learning-based power system dynamic security assessment models under adversarial examples. IEEE Trans Control Network Syst. https://doi.org/10.1109/TCNS.2022.3145285.
36. Ghafari C (2016) Innovative numerical protection relay design on the basis of Sampled Measured Values for Smart Grids. PhD Thesis, Universite Grenoble Alpes.
37. Technical Committee TC 57—Power systems management and associated information exchange, International Electrotechnical Commission, "IEC 61850–7–2, Communication networks and systems for power utility automation –Part 7–2". Basic information and communication structure—Abstract communication service interface (ACSI). IEC Standards Library, February 2020.
38. Technical Committee TC 57—Power systems management and associated information exchange, International Electrotechnical Commission, "IEC 61850-8-5, Communication networks and systems for power utility automation—Part 5". Communication requirements for functions and device models. IEC Standards Library, March, 2022.
39. Technical Committee TC 57—Power systems management and associated information exchange, International Electrotechnical Commission, "IEC 61850-5". Communication networks and systems for power utility automation—Part 90-5: Use of IEC 61850 to transmit synchrophasor information according to IEEE C37.118. Technical Report. IEC Standards Library, May, 2012.
40. System Protection and Control Subcommittee, "Protection System Response to Power Swings", North American Electric Reliability Corporation (NERC), August 2013.
41. IEC 61850-7-1, Communication networks and systems for power utility automation—Part 7–1: Basic communication structure—Principles and models.
42. Ivanković I, Terzija V, Skok S (2018) Transmission network angle stability protection based on synchrophasor data in control centre. J Energy Special Issue 67(3). Papers from 47. CIGRE Session, 26–31, Paris/France, August 2018. https://doi.org/10.37798/EN2018673